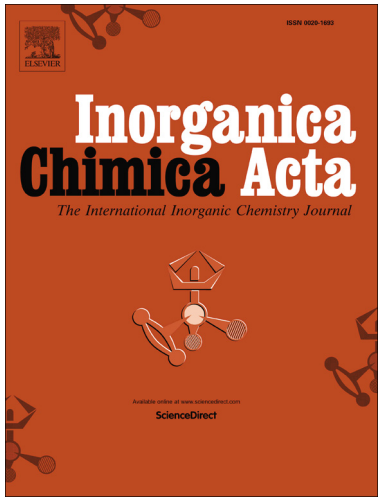


Research paper

# A highly sensitive and selective novel fluorescent chemosensor for detection of $Cr^{3+}$ based on a Schiff base

Gholam Babaei Chalmardi, Mahmood Tajbakhsh, Ahmadreza Bekhradnia, Rahman Hosseinzadeh

PII: S0020-1693(17)30465-6
DOI: http://dx.doi.org/10.1016/j.ica.2017.03.041
Reference: ICA 17501

To appear in: *Inorganica Chimica Acta*

Received Date: 24 March 2017
Accepted Date: 28 March 2017

Please cite this article as: G.B. Chalmardi, M. Tajbakhsh, A. Bekhradnia, R. Hosseinzadeh, A highly sensitive and selective novel fluorescent chemosensor for detection of $Cr^{3+}$ based on a Schiff base, *Inorganica Chimica Acta* (2017), doi: http://dx.doi.org/10.1016/j.ica.2017.03.041

# A highly sensitive and selective novel fluorescent chemosensor for detection of $Cr^{3+}$ based on a Schiff base

**Gholam Babaei Chalmardi[a], Mahmood Tajbakhsh[a]*, Ahmadreza Bekhradnia[b]*, Rahman Hosseinzadeh[a]**

[a] Department of Organic Chemistry, Faculty of Chemistry, University of Mazandaran, Babolsar 47416-95447, Iran
[b] Pharmaceutical Sciences Research Center, Department of Medicinal Chemistry, Mazandaran University of Medical Sciences, Sari, Iran

E-mail: Mahmood.Tajbakhsh32@gmail.com, abekhradnia@gmail.com

## Graphical Abstract

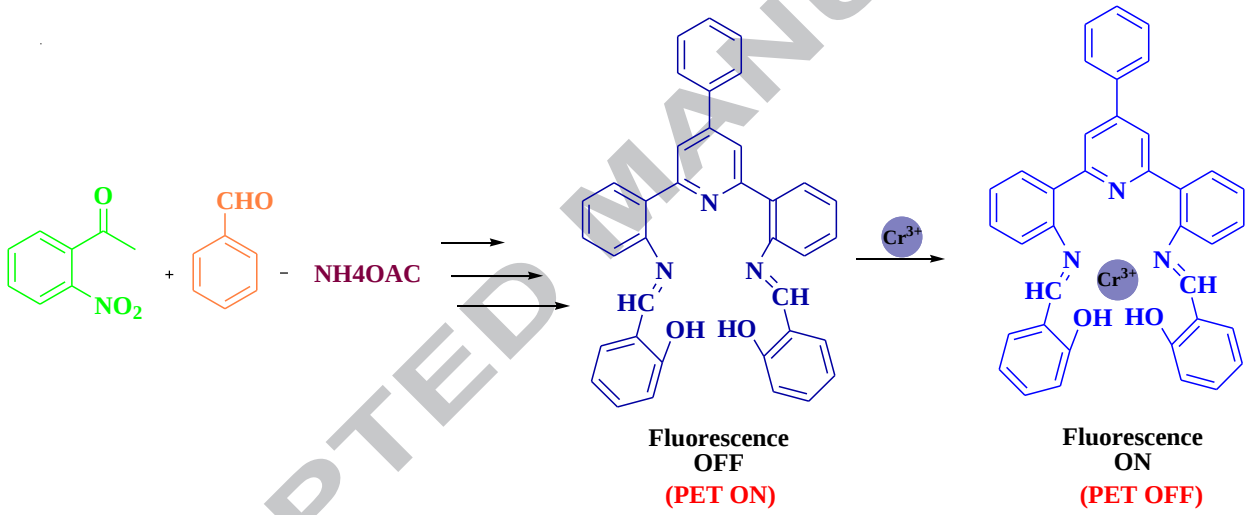


## Highlights

- Synthesis of efficient Schiff base (**3**) as a $Cr^{3+}$ ion fluorescence detector.
- Theoretical study together with Job's plot method showed 1:1 binding ratio of $Cr^{3+}$ with Schiff base **3**.
- The sensing mechanism are explained by photoinduced electron transfer (PET) and chelation - enhanced fluorescence (CHEF).
- It has high affinity ($K_a$ =8.77×10$^4$ $M^{-1}$) and selectivity for $Cr^{3+}$.

- The detection limit of sensor (**3**) towards $Cr^{3+}$ is $2.2\times10^{-7}$ M.


## Abstract

*N,N'*-bis(salicylidene)-2-(6-(2-aminophenyl)-4-phenylpyridin-2-yl) (**3**) was synthesized by condensation reaction of 2,6-bis(2-aminophenyl)-4-phenylpyridine and 2-hydroxybenzaldehyde in EtOH and characterized by its melting point, $^{1}H$,$^{13}C$-NMR and molecular mass. The addition of $Cr^{3+}$ ion makes the significant increase of its fluorescent intensity at 537 nm in $CH_3CN/H_2O$ (95/5%), however, other metal ions have almost no influence on the fluorescence. The reason for this phenomenon might be attributed to the formation of a 1:1 stoichiometric **3**-$Cr^{3+}$ complex which inhibits photo-induced electron transfer (PET) process. The 1:1 binding stoichiometry between **3** and $Cr^{3+}$was established using Job's plot, and the complex structure was proposed by DFT calculation. The association constant ($K_a$) was determined to be $8.77\times10^{4}$ $M^{-1}$ and the limit of detection (LOD) was calculated to be $2.2\times10^{-7}$ M.


**Keywords:** Fluorescence, Chemosensor, Chromium ion, DFT, PET, Schiff base

### 1. Introduction

Complexation of metal ions with specific ligands causing an induce changed in fluorescence are particularly attractive for development of fluorescent chemosensors for metal ions, due to their simplicity, high sensitivity, and rapid response [1]. Selective detection of chromium ion is very important as it is an essential component of a balanced human and animal diet, amounting 50-200 mg per day [2]. Excessive chromium reported to cause genotoxic whereas deficiency of chromium can increase the risk factors associated with diabetes and cardiovascular diseases [3]. Furthermore, chromium is one of the most notorious environmental pollutants [4]. Therefore developments of selective chemosensors for chromium ion are

interesting in environmental and biological fields. Many analytical methods such as X-ray, HPLC, DPP and ICP-AES have been applied for determination of $Cr^{3+}$ ion, but they are usually of high cost and inconvenient for routine analysis. Thus, it is attractive to introduce a more convenient, faster, and lower cost method for trace $Cr^{3+}$ detection, for instance, analyzing by ion-selective sensors [5-11]. Formation of stable complexes of Schiff base with transition metal ions and their application as ion carriers are well known. The host-guest complexion of Schiff bases with metal ions can produce remarkable selectivity, sensitivity and stability for a specific ion. Schiff bases with N, O or S as donor atoms form strong complexes with transition metal ions that can be used as the ionophore in optical sensors for detection of various cations. Schiff base complexes have been widely used in the area of ionic binding, as these binding sites can recognize the metal ions [12-19]. Several publications have reported the use of Schiff base ligands for optical sensing of cations [20-25]. Different mechanisms have been proposed for designing fluorescent chemosensors including chelation-enhanced fluorescence (CHEF) effect, excited state intermolecular proton transfer (ESIPT), photoinduced proton transfer (PPT), metal to ligand charge transfer (MLCT), internal charge transfer (ICT), C=N isomerization and photoinduced electron transfer (PET) [26-31]. As, $Cr^{3+}$ has been known as one of the most efficient fluorescence quenchers [32, 33], its detection via chelation enhanced fluorescence (CHEF) mechanism is an attractive task. Furthermore, due to the lack of selective ionophore, only few turn-on fluorescent sensors for $Cr^{3+}$ have been reported [34]. Herein we report a new fluorescent probe with mixed nitrogen, oxygen donor sites as fluorophore **3** exhibiting a distinct fluorescence enhancement in the presence of $Cr^{3+}$ which forming a 1:1 **3**-$Cr^{3+}$ complex which can inhibit photo-induced electron transfer (**PET**) process. Other metal ions do not induce significant fluorescence changes.

## 2. Experimental

### *2.1. General and reagents*

Melting points were measured on an Electrothermal 9100 apparatus. $^{1}H$ and $^{13}C$ spectra were measured with Bruker DRX-400 AVANCE spectrometer at 400.1 and 100.6 MHz, respectively. Mass spectra were obtained on an Agilent 5975c spectrometer operating at 70 eV. The UV-Vis spectra were obtained using a Perkin-Elmer lambda-EZ 201 and a Jasco FP-200 spectrafluorometer was used to record fluorescence emission spectra. Data were recorded on-line and analyzed by Excel software on a PC computer. Fluorescence intensity measurements were performed at room temperature in solvent $CH_3CN/H_2O$ (95/5%).

### *2.2. Synthesis*

#### *2.2.1. Synthesis of 2,6-bis(2-nitrophenyl)-4-phenylpyridine(**1**)*

This compound was synthesized according to reported Procedure [35]. Typically in a round-bottomed flask (250 mL) equipped with a reflux condenser, a mixture of benzaldehyde (6.4 g, 0.06 mol), 2′-nitroacetophenone (20 g, 0.12 mol), ammonium acetate (60 g), and glacial acetic acid (150 ml) was refluxed for 2 h. Upon cooling, crystals separated, which were filtered and washed first with acetic acid (50%) and then with cold ethanol. The dark yellow crystals were recrystallized from absolute ethanol, and dried at 60 ºC under vacuum (Scheme1). Yield: 66%, mp 188-191 ˚C, $^{1}H$ NMR (400 MHz, $CDCl_3$), δ, ppm: 7.94 (2H, d, J =8Hz), 7.72-7.74 (3H, m), 7.70-7.71 (m, 2H), 7.68-7.69 (3H, m), 7.56-7.60(2H, m), 7.51-7.536(2H, m), 7.51-7.53 (2H, m). $^{13}C$ NMR (100 MHz, $CDCl_3$), δ, ppm: 155.82, 150.43, 149.16, 137.60, 134.99, 132.73, 131.68, 129.53, 129.46, 129.25, 127.31, 124.42 and 120.16. The mass spectrum showed the molecular peak at m/z = 397.1 corresponding to compound **1**(Fig. S1-S2).

*2.2.2. Synthesis of 2,6-bis(2-aminophenyl)-4-phenylpyridine(**2**)*

In a two-necked round-bottomed flask (500 ml) equipped with a reflux condenser and a dropping funnel, a suspension of 2,6-bis(2-nitrophenyl)-4-phenylpyridine (13.75 g, 0.033 mol), palladium on carbon 5% (1.4 g), and ethanol (500 mL) was prepared. The mixture was warmed, and while being stirred magnetically, hydrazine hydrate 85% (35 ml) in ethanol (50 ml) was added dropwise over 1.5 h period through the dropping funnel while maintaining the temperature at about 50 ºC. The reaction mixture was then refluxed for 2 h and filtered while hot. On cooling, the filtrate gave white-cream colored crystals of the title diamine compound, which was recrystallized from ethanol and vacuum dried (Scheme1). Yield: 68%, mp 167-169 ˚C,$^{1}$H NMR (400 MHz, $CDCl_3$), δ, ppm:7.76 (2H, d, J=2.4Hz), 7.73 (2H, d, J=1.2Hz), 7.62 (2H, dd, J=1.6Hz, J=7.2Hz), 7.53-7.57 (2H,m), 7.49-7.51 (1H, m), 7.23 (2H, Td, J=1.6Hz, J=7.6Hz), 6.85 (2H, Td, J=0.8 Hz, J=7.6 Hz), 6.8(2H, dd, J=0.8, J=8.4Hz), 5.41(4H, s, $NH_2$). $^{13}$C NMR (100 MHz, $CDCl_3$), δ, ppm: 158.22, 150.67, 146.10, 138.90, 129.98, 129.87, 129.15, 129.06, 127.18, 123.18, 118.64, 117.81 and 117.032. The mass spectrum showed the molecular peak at m/z = 336.1 corresponding to compound **2** (Fig. S3-S4).

*2.2.3. N,N'-bis(salicylidene)-2,6-bis(2-aminophenyl)-4-phenylpyridine(**3**)*

A solution included 2,6-bis(2-aminophenyl)-4-phenylpyridine(1 mmol) in absolute ethanol was added to an ethanol solution of 2-hydroxybenzaldehyde (2 mmol). The mixture was refluxed for 8 h and then cooled to room temperature. Then, the solvent was evaporated and the yellow product was recrystallized from ethanol (Scheme1). Yield: 88%, mp 221-224 ˚C, $^{1}$H NMR (400 MHz, $CDCl_3$), δ, ppm:12.97 (2H, s), 8.69 (2H, s), 7.76 (2H, dd, J=1.2Hz, J=7.6Hz), 7.69 (2H, s), 7.63-7.65 (2H, m), 7.39-7.47 (6H, m), 7.34-7.37 (3H, m), 7.22–7.26 (4H, m), 6.97 (3H, d, J=8Hz), 6.94 (1H, d, J=0.8Hz). $^{13}$C NMR (100 MHz, $CDCl_3$), δ, ppm: 163.72, 160.97,

157.21, 148.78, 147.03, 138.66, 135.01, 133.23, 132.39, 131.22, 129.67, 128.86, 128.67, 127.48, 126.90, 121.69, 119.43, 119.16, 119.05 and 117.22. The mass spectrum showed the molecular peak at m/z = 545.3 corresponding to compound **3** (Fig. S5-S6).

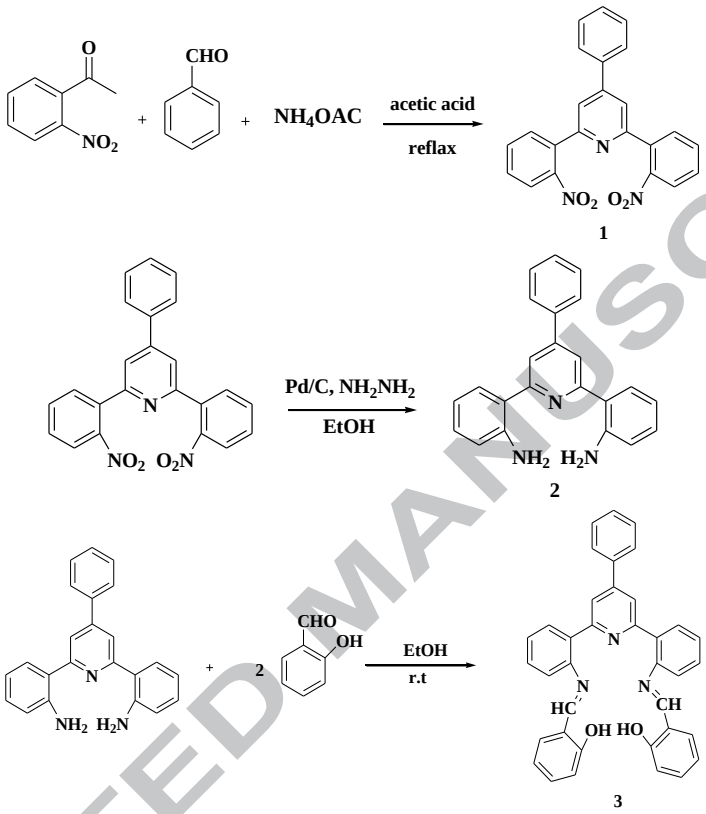


**Scheme. 1.** The synthetic route for compound **3**.

*2.3. Spectrometric procedure*

The stock solutions of nitrate salts (10 μM) of $Na^{+}$, $Ag^{+}$, $K^{+}$, $Ca^{2+}$, $Pb^{2+}$ , $Hg^{2+}$, $Mn^{2+}$, $Co^{2+}$, $Cu^{2+}$, $Zn^{2+}$, $Cd^{2+}$, $Fe^{3+}$,$Cr^{3+}$ and $Al^{3+}$ in $CH_3CN/H_2O$ (95/5%) were prepared. Another solution comprises compound **3** was dissolved in acetonitrile (10 μM). Then 2 mL of each (2mL of compound **3**+2 mL of nitrate salt solution) were added to the measurement cell. For all measurements, excitation wavelength was at 273 nm at room temperature.

## 3. Results and discussion

### *3.1. Spectral studies*

Fig. 1 and 2 show changes in the absorption and fluorescence spectra in $CH_3CN/H_2O$ (95/5%) of **3**, upon the addition of various cations salts. The absorption spectrum of **3** (10 μM) in $CH_3CN/H_2O$ (95/5%) solution exhibits three bands at 212 nm, 273 nm and 333 nm. The absorption intensity of compound **3** decreased with the addition of various metal ions e.g. $Cr^{3+}$, $Na^{+}$, $Ag^{+}$, $K^{+}$, $Ca^{2+}$, $Pb^{2+}$ , $Hg^{2+}$, $Mn^{2+}$, $Co^{2+}$, $Cu^{2+}$, $Zn^{2+}$, $Cd^{2+}$, $Fe^{3+}$, $Al^{3+}$. The cations studied led to hypochromic effects in absorbance in the UV-Vis spectra of **3** (Fig. 1). By UV-Vis analysis, it was difficult to identify specific cations over other metal ions because of the ambiguous absorption spectra [36]. Therefore, to investigate the selectivity of **3** for $Cr^{3+}$ in the presence of other metal ions, the fluorescence response of **3** toward various metal ion solutions (10 μM) was studied in $CH_3CN/H_2O$ (95/5%) (Fig. 2)

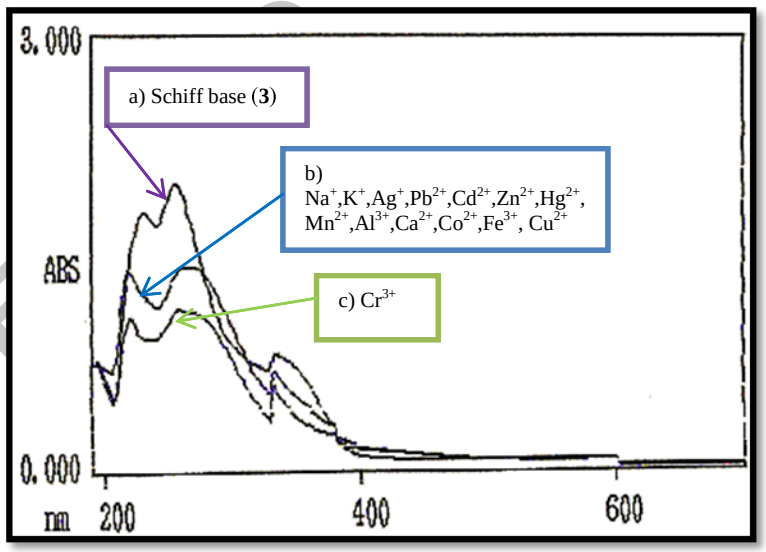


**Fig. 1.** Absorption spectra of Schiff base **3** (10 μM) before (a) and after addition of heavy metal mixtures (2 equiv) in the absence of $Cr^{3+}$ (b) and heavy metal mixtures in the presence of $Cr^{3+}$ in $CH_3CN/H_2O$ (95/5%) solution. (c).

The fluorescence emission intensity of **3** was recorded at 537 nm when it was excited at 273 nm. Upon addition of $Cr^{3+}$, **3** shows a large fluorescence enhancement due to the formation of a 1:1 **3**-$Cr^{3+}$ complex which inhibits photo-induced electron transfer (**PET**) process [37-39].

Other metal ions including $Na^{+}$, $Ag^{+}$, $K^{+}$, $Ca^{2+}$, $Pb^{2+}$ , $Hg^{2+}$, $Mn^{2+}$, $Co^{2+}$, $Cu^{2+}$, $Zn^{2+}$, $Cd^{2+}$, $Fe^{3+}$ and $Al^{3+}$ have almost no influence on the fluorescence, which indicated the Schiff base (**3**) that is a highly selective fluorescent sensor for $Cr^{3+}$.

**a)**

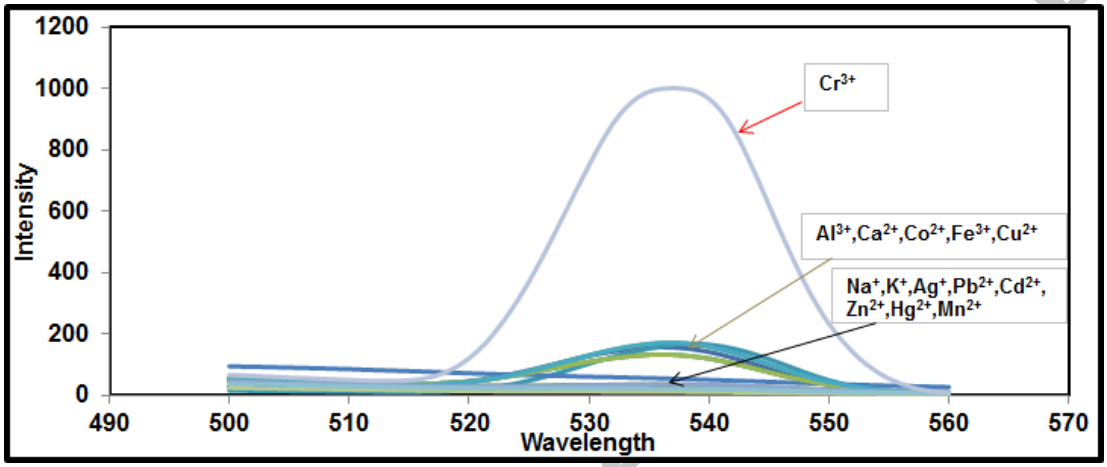


**b)**

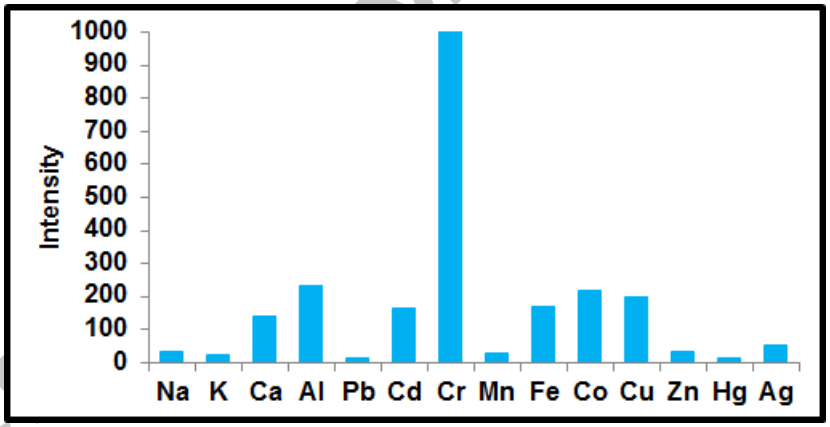


**Fig. 2.** (a) Fluorescence responses of compound **3** (10 μM) in $CH_3CN/H_2O$ (95/5%) solution upon the addition of various metal ions (λex = 273nm, 2 equiv). (b) Bar graph representing the change of the relative emission intensity of **3** at 537 nm upon treatment with various metal ions (λex = 273 nm).

The addition of $Cr^{3+}$ ion to a mixture of **3** and the other potentially competitive metal ions mentioned above in a $CH_3CN/H_2O$ (95/5%) solution, led to an enhancement of fluorescence intensity (Fig. 3). These observations demonstrate that Schiff base **(3)** could be used as an efficient and selective fluorescence chemosensor for $Cr^{3+}$ ion.

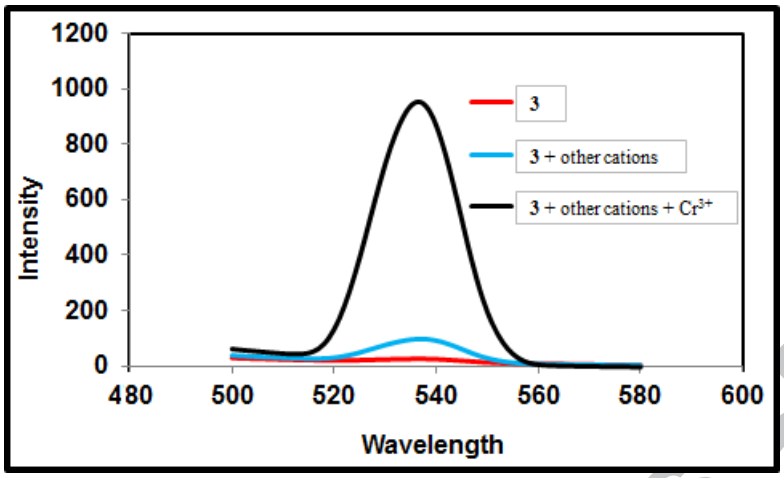


**Fig. 3.** Fluorescence intensity of **3** (10 μM) in the absence of metal ions (red curve), and presence of 2 equiv of all kinds of competitive metal ions (blue curve) in $CH_3CN/H_2O$ (95/5%, λex = 273 nm). The black curve represents the addition of $Cr^{3+}$ to the above mixture. Each spectrum was acquired 1 minute after cations addition at room temperature.

To further confirm the properties of receptor **3** as a sensor for $Cr^{3+}$ ion titrations were performed by adding of $Cr^{3+}$ to the solutions of sensor **3** in $CH_3CN/H_2O$ (95/5%) solvent (Fig. 4).

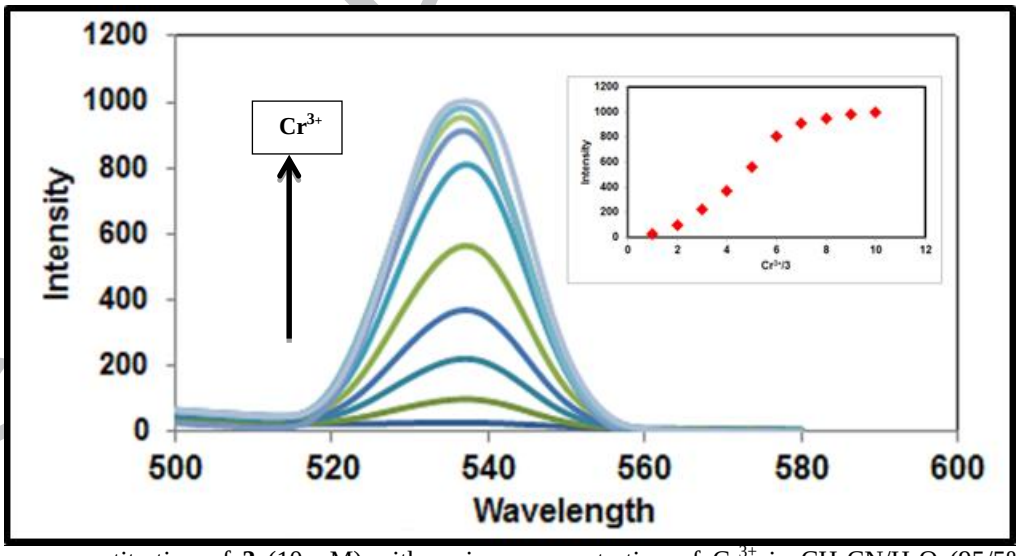


**Fig.4.** Fluorescence titration of **3** (10 μM) with various concentration of $Cr^{3+}$ in $CH_3CN/H_2O$ (95/5%) solution (excitation = 273 nm) at room temperature. inset: changes of fluorescence upon addition of $Cr^{3+}$ (0-2 equiv) at emission=537 nm.

The association constant ($K_a$) of compound **3** with metal ions was determined using the Benesi–Hildebrand equation [40], as follows:

$$\frac{1}{F - F_0} = \frac{1}{K_a(F_{max} - F_0)[M]} + \frac{1}{F_{max} - F_0}$$

F and $F_0$ represent the fluorescent intensity of compound **3** in the presence and absence of metal ions, respectively. $F_{max}$ is the saturated fluorescent intensity of compound **3** in the presence of excess amount of metal ions that [M] is the concentrate ion of added metal ions. According to Benesi–Hildebrand equation, the association constant between receptor **3** and $Cr^{3+}$ was calculated from the fluorescence titration result and was found to be $8.77\times10^4$ $M^{-1}$. Moreover, the detection limit was calculated based on the fluorescence titration. To determine the S/N ratio, the emission intensity of the complex (**3**-$Cr^{3+}$) was measured and the standard deviation of blank measurements was calculated. The detection limit was then calculated according to 3 × δb/m. where δb was the standard deviation of blank solutions, and m was the slope between intensity vs. sample concentration [41]. The detection limit for $Cr^{3+}$ was calculated to $2.2\times10^{-7}$ mol/L. Fluorescence quantum yield was determined by comparing the emission and absorption intensities of the probe with those of a fluorescence standard, fluorescein in 0.1 N NaOH [42]. For all fluorescence measurements, the excitation wavelength was 273 nm with excitation and emissions slit widths of 3.0 nm. Quantum yield of 15.9% was calculated for the **3**-$Cr^{3+}$complex. Nevertheless, low quantum yields were obtained for combined receptor and other cations as well as free receptor and no worth to report.

*3.2. Binding mode studies*

In order to determine the stoichiometry of the Schiff base (**3**) with $Cr^{3+}$complex, the method of continuous variation (Job's plot) was used. The total concentration of the complex **3**-$Cr^{3+}$was constant (10 µM), with a continuous variable molar fraction of guest ([**3**]/[ $Cr^{3+}$] + [**3**]). Fig. 5

shows the Job plot of Schiff base **3** with $Cr^{3+}$ (at 537 nm), the **3**-$Cr^{3+}$ complex concentration approaches a maximum when the molar fraction of $Cr^{3+}$ is 0.5, confirming that **3** and $Cr^{3+}$ forms a 1:1 complex.

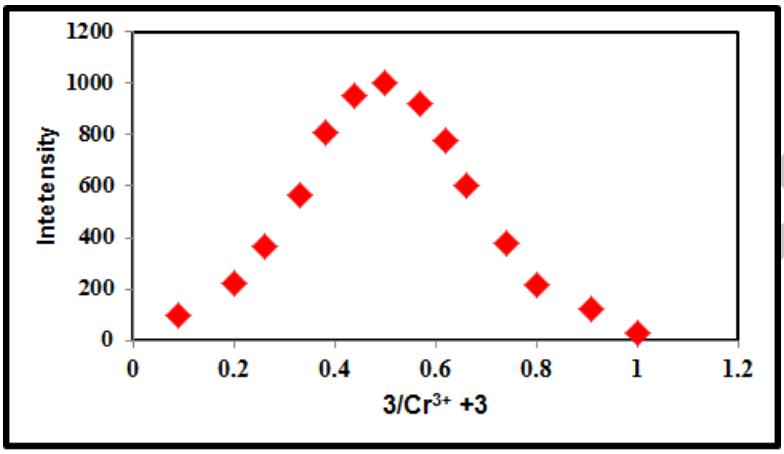


**Fig. 5.** Job's plot for determining the stoichiometric complexation of **3** with $Cr^{3+}$ in $CH_3CN/H_2O$ (95/5%) at room temperature. The total concentration of **3** and $Cr^{3+}$ is 10 µM.

To understand the complexation between the compound **3** and $Cr^{3+}$, the $^1H$ NMR titration experiments were conducted by addition increasing concentrations of $Cr^{3+}$ upon the **3** solution. As is seen in (Fig. 6), the OH signal ($H_a$) of **3** appeared at δ 12.96 ppm. But after addition of 2.0 equiv of $Cr^{3+}$ to the **3** solution this signal was disappeared which means that phenolic OH group may be deprotonated and this implies that the phenolic OH group is efficient on formation of complex between the **3** and $Cr^{3+}$. The imine proton ($H_b$) of **3** at around δ 8.69 ppm decreased on addition of $Cr^{3+}$ to the **3** solution. It indicates that the nitrogen atom of the Schiff base **3** may participate in coordination with $Cr^{3+}$ ions. In addition, the protons of benzene rings were decreased. For instance, $H_c$ and $H_d$ were affected due to complex formation. This observation may imply that phenolic OH group and imine moiety efficient on the formation of complex between **3** and $Cr^{3+}$ [43].

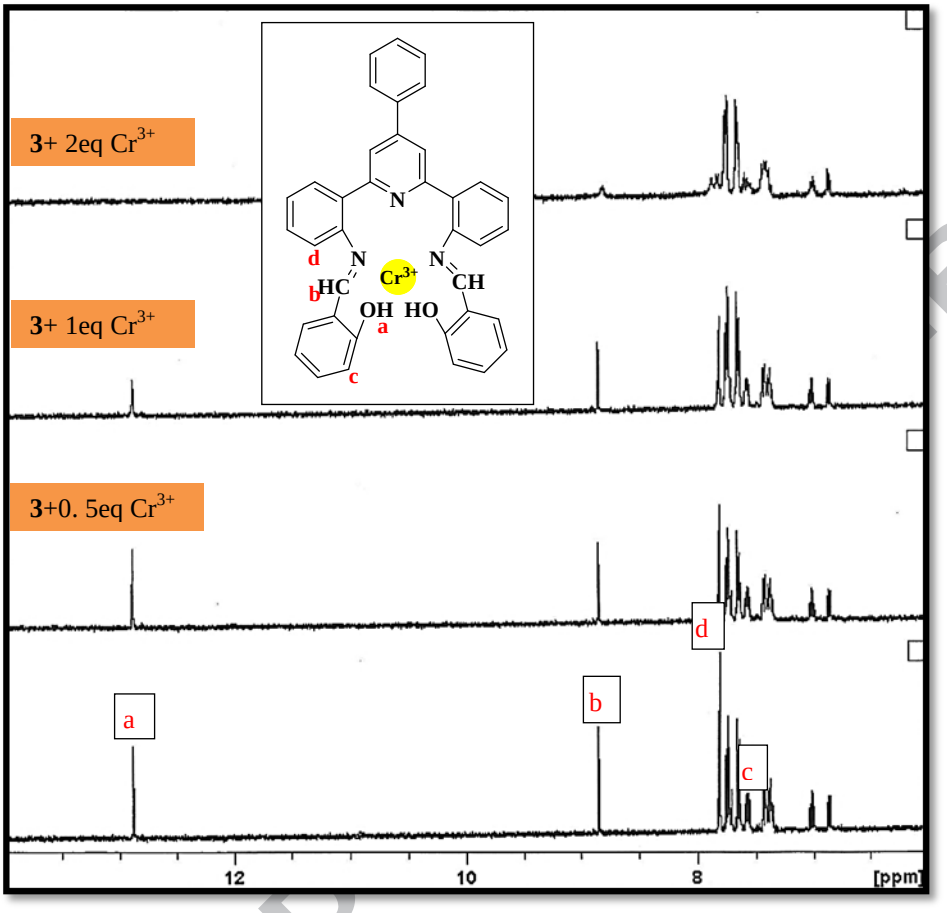


**Fig. 6.** Partial $^{1}$H NMR spectra of **3** (10 µM) in $CD_3CN$ at room temperatureand the corresponding changes after the addition of increasing amounts of Chromium nitrate (0-2 equiv). Each spectrum was acquired 1 minute after $Cr^{3+}$ addition at room temperature.

*3.3. Theoretical study*

The complex (**3**-$Cr^{3+}$) gave fine powders and we were not able to prepare single crystals for structure determination by X-ray spectroscopy [25]. Instead, to get insight into the proposed binding mode, full geometry optimizations were performed without any symmetry constraints by means of hybrid functional $B_3LYP$ and the 6–311G* basis set, employing the Gaussian package. The optimized geometry and the highest occupied molecular orbital (HOMO) and lowest unoccupied molecular orbital (LUMO) of **3** and its $Cr^{3+}$ complex are presented in (Fig. 7 and Fig. S7-S8).

a)

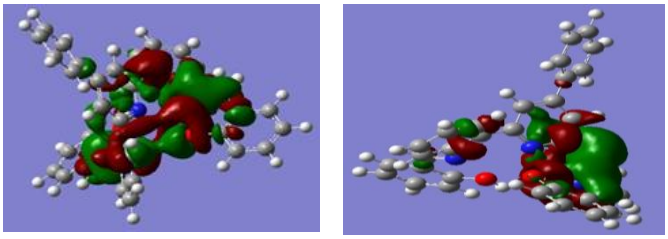

LUMO HOMO-4

b)

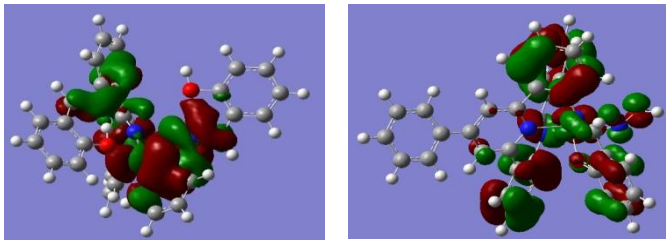

LUMO HOMO-4

**Fig. 7.** DFT Optimized structure of HOMO and LUMO orbitals of a) **3** and b) **3**-$Cr^{3+}$ complex.

To attain a deeper insight into the UV-Vis analysis, the TDDFT calculations of free ligand **3**, was performed with the comparable studies. The obtained UV-Vis spectra by means of TDDFT calculation were confirmed by experimental UV-Vis spectroscopy (Fig. S9). From the Density Functional Theory (DFT) calculations, $\lambda_{max}$ of **3** and **3**-$Cr^{3+}$ were obtained by 273 nm, which are confirmed by the experimental results. The results of TDDFT have interesting coincidence with the obtained UV-Vis achievements (Fig. S9 and Fig. 8).

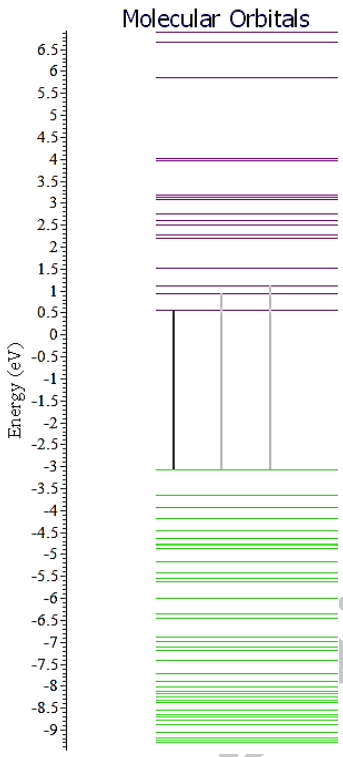


**Fig. 8.** Molecular Orbitals of **3**, HOMO (green) and LUMO (red).

In **3**, the contributions of HOMO-2 to LUMO+2, HOMO-3 to LUMO+1, HOMO-4 to LUMO transitions were 12.96%, 27% and 3.61%, respectively. Due to the importance of the lone pair electrons of the nitrogen atom, we carefully analysed its contribution to the relevant orbitals. It was found that the nitrogen lone pair electron belongs to HOMO-4 in **3**. Thus, HOMO-4→LUMO transition (3.61%) is responsible for the fluorescence quenching. On the other hand, in **3**-$Cr^{3+}$, the nitrogen atom has strong interaction with $Cr^{3+}$ d-orbital to produce bonding type orbitals that block the PET process from the nitrogen lone pair electron to the benzene, hence block the fluorescence quenching. The possibility of the restricted chelation-enhanced fluorescence (CHEF) process of **3** on coordination to $Cr^{3+}$ could also contribute to the fluorescence enhancement along with the PET process [44] (Scheme 2 and Fig. 9).

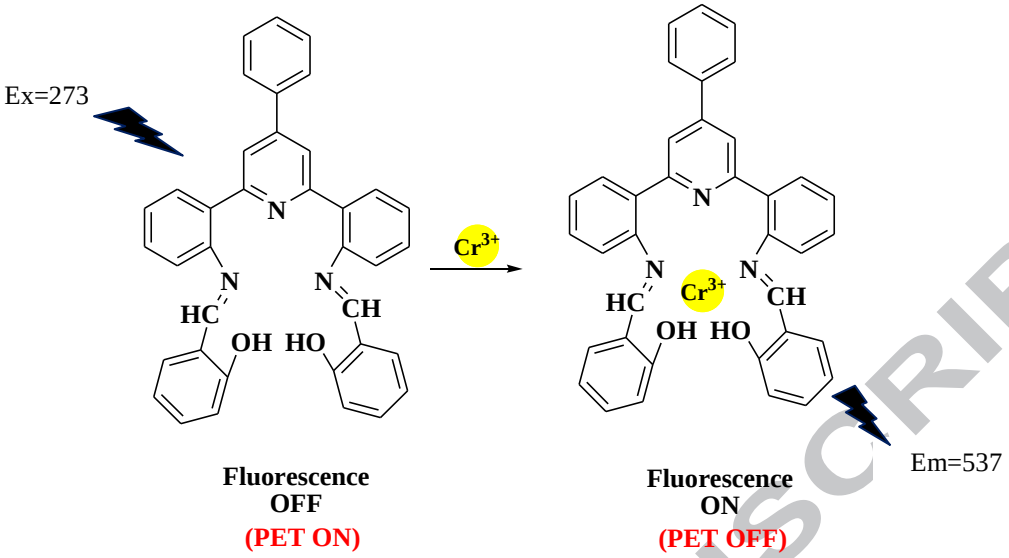


**Scheme. 2.** Proposed mechanism for detection of $Cr^{3+}$ by **3.**

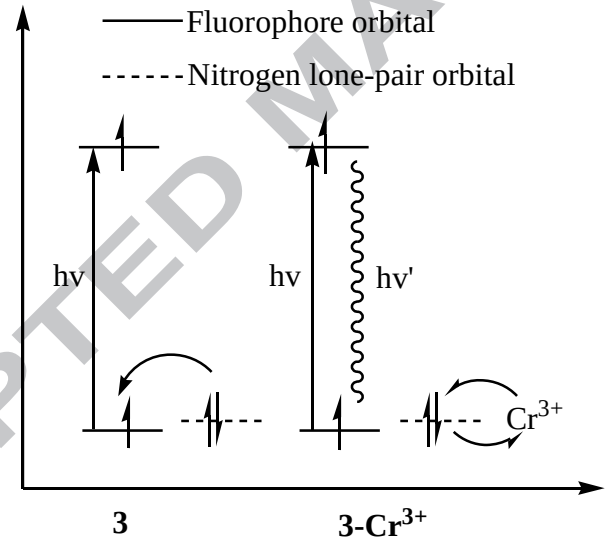


**Fig. 9.** Proposed mechanism of fluorescence enhancement.

In order to show of proposed reliability our suggestion mechanism and to improve the accuracy in estimating energy levels of occupancy orbitals, we have found all the related molecular orbitals of ligand **3** using TDDFT theory. Our computational results showed the fluorescence enhancement by the $Cr^{+3}$ could be rationalized in the sense of the HOMO-LUMO gap. The output diagram of our calculation was depicted in Fig.8 it was seen, that energy gap

between HOMO-4 and LUMO is 5 eV ($8.0\times10^{-19}$ j). Noticeably, in our experiments the excitation wavelength for ligand 3 was found 273 nm which related to 4.6 eV ($7.3\times10^{-19}$ j) gap. Those results have showed that our experimental data are consistence with theoretical outcome. Thus, the results of the DFT calculations further corroborate the proposed sensing mechanism.

As depicted in Fig. 10 and Table 1, sensor **3** forms a 1:1 complex with $Cr^{3+}$. Furthermore, $Cr^{3+}$ has favourable interactions with the two oxygen atoms of hydroxyl groups and the two nitrogen atoms of two amine groups and two oxygen atoms of a nitrate of the sensor [45, 46]. Then, the structural parameters of **3** changed slightly upon addition of $Cr^{3+}$ and formed **3**-$Cr^{3+}$ as the dihedral angle $N_{26}$-$O_{42}$-$N_{25}$-$O_{41}$ was 19.763 in 3 and 24.466 in **3**-$Cr^{3+}$. Moreover, the distance between $N_{10}$ and $Cr_{43}$ is 2.149 Å which indicates that no bond is formed between two atoms.

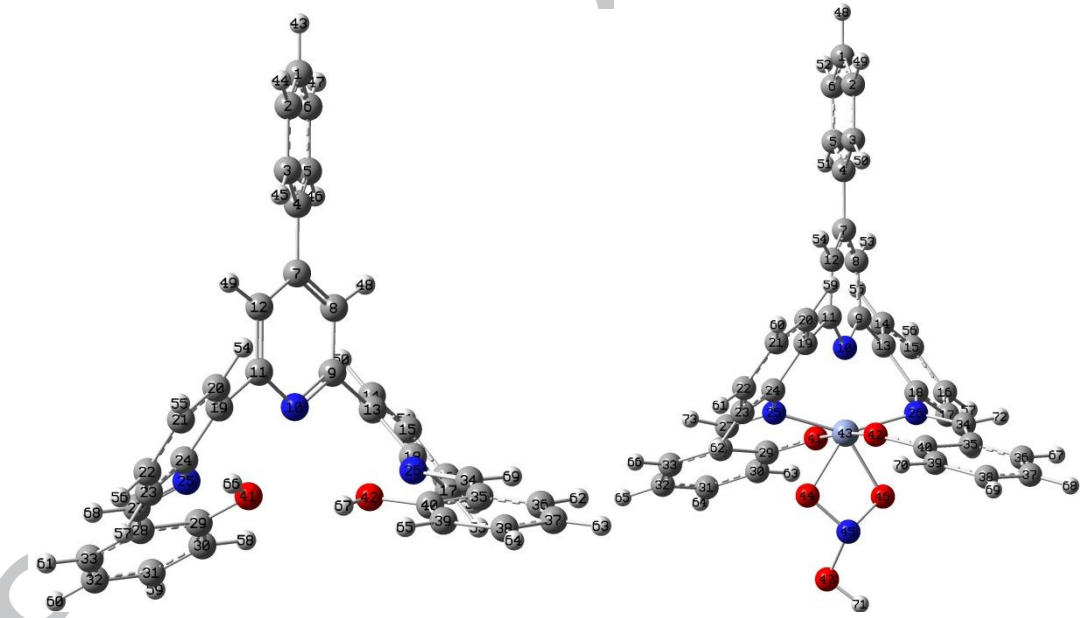

(a) (b)

**Fig. 10.** Optimized structure of a) **3** and b) **3**-Cr (III) by DFT.

**Table 1**
The selected bond lengths (Å) and angles (°) for **3**-Cr (III).

| Bond length (Å) | | Bond angle (°) | | Dihedral angle(°) | |
|---|---|---|---|---|---|
| $Cr_{43}$-$N_{25}$ | 1.998 | $N_{25}$-$Cr_{43}$-$N_{26}$ | 150.237 | $N_{26}$-$O_{42}$-$N_{25}$-$O_{41}$ | 24.466 |
| $Cr_{43}$-$N_{26}$ | 1.997 | $N_{25}$-$Cr_{43}$-$O_{41}$ | 89.387 | $O_{42}$-$O_{46}$-$O_{44}$-$O_{41}$ | 103.064 |
| $Cr_{43}$-$O_{41}$ | 1.901 | $N_{25}$-$Cr_{43}$-$O_{44}$ | 70.267 | $C_{29}$-$O_{41}$-$Cr_{43}$-$N_{26}$ | 177.883 |
| $Cr_{43}$-$O_{42}$ | 1.902 | $N_{25}$-$Cr_{43}$-$O_{46}$ | 138.580 | $C_{40}$-$O_{42}$-$Cr_{43}$-$N_{25}$ | 178.643 |
| $Cr_{43}$-$O_{44}$ | 1.922 | $N_{25}$-$Cr_{43}$-$O_{42}$ | 92.334 | $C_{24}$-$N_{25}$-$Cr_{43}$-$O_{42}$ | 18.462 |
| $Cr_{43}$-$O_{46}$ | 1.925 | $N_{26}$-$Cr_{43}$-$O_{42}$ | 89.460 | $C_{18}$-$N_{26}$-$Cr_{43}$-$O_{41}$ | 19.786 |
| | | $N_{26}$-$Cr_{43}$-$O_{41}$ | 91.413 | $C_{27}$-$N_{25}$-$Cr_{43}$-$N_{26}$ | 119.200 |
| | | $N_{26}$-$Cr_{43}$-$O_{46}$ | 70.971 | $C_{34}$-$N_{26}$-$Cr_{43}$-$N_{25}$ | 119.984 |
| | | $N_{26}$-$Cr_{43}$-$O_{44}$ | 139.437 | $C_{28}$-$C_{29}$-$O_{41}$-$Cr_{43}$ | 22.288 |
| | | $O_{41}$-$Cr_{43}$-$O_{42}$ | 174.925 | $C_{35}$-$C_{40}$-$O_{42}$-$Cr_{43}$ | 21.895 |
| | | $O_{41}$-$Cr_{43}$-$O_{44}$ | 90.954 | $C_{19}$-$C_{24}$-$N_{25}$-$Cr_{43}$ | 57.832 |
| | | $O_{41}$-$Cr_{43}$-$O_{46}$ | 83.781 | $C_{13}$-$C_{18}$-$N_{26}$-$Cr_{43}$ | 57.637 |
| | | $O_{42}$-$Cr_{43}$-$O_{46}$ | 91.784 | $C_{18}$-$N_{26}$-$Cr_{43}$-$O_{44}$ | 112.907 |
| | | $O_{42}$-$Cr_{43}$-$O_{44}$ | 85.141 | $C_{24}$-$N_{25}$-$Cr_{43}$-$O_{46}$ | 113.816 |
| | | $O_{44}$-$Cr_{43}$-$O_{46}$ | 69.063 | $C_{29}$-$O_{41}$-$Cr_{43}$-$O_{46}$ | 107.198 |
| | | | | $C_{40}$-$O_{42}$-$Cr_{43}$-$O_{44}$ | 108.678 |

*3.4. Solvent effect*

Optical sensing nature of chemosensors was found to be depended on the solvent nature, so the response of ligand **3** toward $Cr^{3+}$ ion was also examined in different solvents such as DMSO, DMF, methanol, acetonitrile, acetonitrile/$H_2O$ at maxima of emission intensity. As shown in fig. 11, the optimum fluorescence enhancement occurred both in acetonitrile and acetonitrile/$H_2O$ (95/5%). The aprotic solvents (DMSO, DMF) and protic solvents (methanol, $H_2O$) decrease significant the intensity of fluorescent, which might be due to hydrogen bonding of this solvents with hydroxyl groups, rather than general solvent effects [47]. However, the highest fluorescent intensity was observed in acetonitrile and acetonitrile/$H_2O$ (95/5%). So acetonitrile/$H_2O$ (95/5%) was chosen as solvent [48].

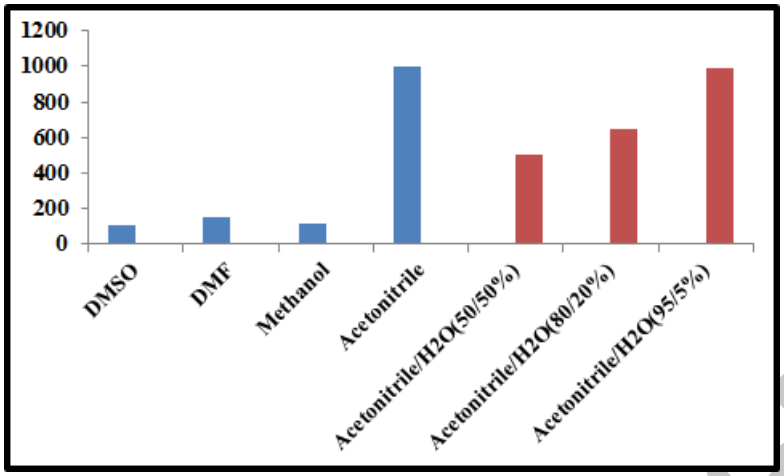


**Fig. 11.** Solvent effect on fluorescent intensity of **3** (10 µM) with $Cr^{3+}$ (2 equiv) in different solvent DMSO, DMF, methanol, acetonitrile, acetonitrile/$H_2O$ (50/50%), acetonitrile/H2O (80/20%), acetonitrile/H2O (95/5%).

*3.5. Effect of pH on the binding affinity of $Cr^{3+}$ to **3***

Since pH of the medium plays a crucial role in fluorescence detection, the effect of pH in the range of (2–13) on the fluorescence response of **3** was investigated in $CH_3CN/H_2O$ (95/5%) mixture. The changes in the fluorescence intensity at 537 nm of **3** in the absence and presence of $Cr^{3+}$ ion were plotted as a function of pH (Fig. 12). The overall fluorescence intensity of **3**–$Cr^{3+}$ remained higher than the free receptor **3**. Fluorescent intensity was found to be the highest at pH 8. Beyond pH 8 $Cr^{3+}$ might be transformed into $Cr(OH)_3$, removed from **3**, thus the emission intensity decreased. Similarly below pH 8 **3** might combine with $H^+$ and show no tendency to bind $Cr^{3+}$, which resulting a decrease in fluorescence intensity. Therefore, **3** can tolerate the detection of $Cr^{3+}$ in the pH 8 [49].

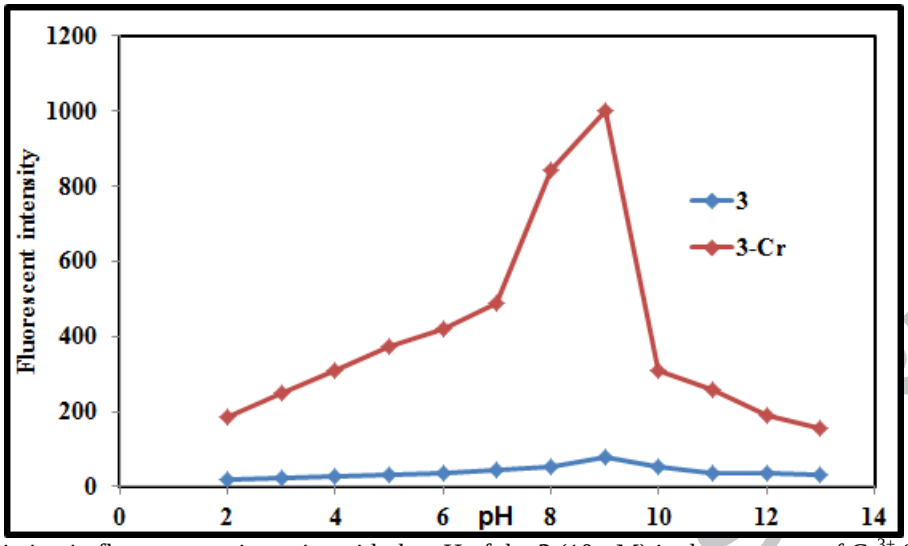


**Fig. 12.** The variation in fluorescence intensity with the pH of the **3** (10 μM) in the presence of $Cr^{3+}$ (2 equiv) at emission wavelength 537 nm.

*3.6. Comparison*

The *N,N'*-bis(salicylidene)-2-(6-(2-aminophenyl)-4-phenylpyridin-2-yl) (**3**) for fluorescence sensing of $Cr^{3+}$ is very interesting. In addition, we compared the present sensor with those previously reported chemosensors for $Cr^{3+}$ (Table 2). Chemosensor **3** exhibited better response relatively.

**Table 2**: Comparative analysis of chemosensor **3** with previously reported sensors.

| Ionophores | mechanism | Methods of detections | Medium of detection | Detection limit (M) | Binding Constant $M^{-1}$ | Sensing response | pH range |
|---|---|---|---|---|---|---|---|
| Ref. 50 | - | fluorescent | $CH_3CN/H_2O$ (8:2) | $7.94 \times 10^{-5}$ | $1.6 \times 10^{4}$ | $Cr^{3+}$ (Turn on) | 7 |
| Ref. 51 | PET | colorimetric and fluorescent | MeOH | $1.21 \times 10^{-6}$ | $1.01\times 10^{4}$ | $Cr^{3+}$ (Turn on) | 2-7 |
| Ref. 52 | - | colorimetric and fluorescent | MeOH | $1.1 \times 10^{-5}$ | $1.4 \times 10^{4}$ | $Cr^{3+}$ (Turn on) | - |
| Ref. 53 | C=N isomerization and ESIPT | colorimetric and fluorescent | $CH_3CN$ | $2.75 \times 10^{-6}$ | $5.97 \times 10^{4}$ | $Cr^{3+}$ (Turn on) | - |
| Ref. 54 | - | fluorescent | $CH_3CN$ | $9.86 \times 10^{-6}$ | $2.1\times 10^{3}$ | $Cr^{3+}$ (Turn on) | 6-8 |
| **3** | PET and CHEF | fluorescent | $CH_3CN/H_2O$ (95/5%) | $2.2\times10^{-7}$ | $8.77\times10^{4}$ | $Cr^{3+}$ (Turn on) | 8 |

## 4. Conclusions

Synthesis of compound **3** can be achieved by the condensation reaction of 2-(6-(2-aminophenyl)-4-phenylpyridin-2-yl)benzenamine with 2-hydroxybenzaldehyde. It possesses a high affinity and selectivity for $Cr^{3+}$ relative to other different competitive metal ions like $Na^{+}$, $Ag^{+}$, $K^{+}$, $Ca^{2+}$, $Hg^{2+}$, $Mn^{2+}$, $Co^{2+}$, $Cu^{2+}$, $Zn^{2+}$, $Cr^{3+}$, $Cd^{2+}$, $Fe^{3+}$, $Al^{3+}$ by enhancement of the fluorescence emission. It is expected that the present design strategy and the remarkable photo physical properties of this chemosensor will help to extend applications of fluorescent chemosensors for metal ions. The results of Job's plot method together with theoretical study indicate that **3** and $Cr^{3+}$ form a 1:1 complex. The association constant $K_a$ was determined to be $8.77\times10^{4}$ $M^{-1}$ and the limit of detection (LOD) was calculated to be $2.2\times10^{-7}$ M exhibiting more efficient than other reported $Cr^{3+}$ sensors [50–54].

References

[1] S. Pawar, U. Fegade,V.K. Bhardwaj, N. Singh, R. Bendre, A. Kuwar, Polyhedron. 87 (2015)79-85.
[2] N.R. Council, Recommended dietary allowances. Food and Nutrition Board, Commission on Life Sciences, National Research Council. Washington: National Academic (1989).
[3] R. McRae, P. Bagchi, S. Sumalekshmy, C.J. Fahrni, Chem. Rev. 109 (2009) 4780-4827.
[4] C. Cervantes, J. Campos-García, S. Devars, F. Gutiérrez-Corona, H. Loza-Tavera, J.C. Torres-Guzmán, R. Moreno-Sánchez, Microbiology Reviews. 25 (2001) 335-347.
[5] V.K. Gupta, A.K. Jain, P. Kumar, S. Agarwal, G. Maheshwari, Sens. Actuators B. 113 (2006) 182-186.
[6] H.A. Zamani, G. Rajabzadeh, M.R. Ganjali, Sens. Actuators B. 119 (2006) 41-46.
[7] A.K. Singh, V.K. Gupta, B. Gupta, Anal. Chim. Acta. 585 (2007) 171-178.
[8] A.J. Weerasinghe, C. Schmiesing, E. Sinn, Tetrahedron Lett. 50 (2009) 6407-6410.
[9] H.W. Wang, Y.Q. Feng, C. Chen, J.Q. Xue, Chin. Chem. Lett. 20 (2009) 1271-1274.
[10] Y. Wan, Q. Guo, X. Wang, A. Xia, Anal. Chim. Acta. 665 (2010) 215-220.
[11] Y. Lei, Y. Su, J. Huo, Spectrochim. Acta A: Mol. Biomol. Spectrosc. 83 (2011) 149-154.
[12] D. Maity, T. Govindaraju, Inorg. Chem. 49 (2010) 7229-7231.
[13] D. Maity, T. Govindaraju, Chem. Commun. 46 (2010) 4499-4501.
[14] R. Azadbakht, J. Khanabadi, Tetrahedron. 69 (2013) 3206-3211.
[15] J.C. Qin, Z.Y. Yang, P. Yang, Inorg. Chim. Acta .432 (2015) 136-141.
[16] W. Ruo, J. Guang-Qi, L. Xiao-Hong, Inorg. Chim. Acta. 455 (2017) 247–253.
[17] C. Bhaumik, D. Maity, S. Das, S. Baitalik, RSC Advances. 2 (2012) 2581–2594.
[18] C. Bhaumik, S. Das, D. Maity, S, Baitalik, Dalton Trans. 40 (2011) 11795-11808.
[19] D. Zhou, C. Sun, C. Chen, X. Cui, W. Li, Journal of Molecular Structure. 1079 (2015) 315–320.
[20] N. Aksuner, E. Henden, I. Yilmaz, A. Cukurovali, Sens. Actuators B. 134 (2008) 510-515.
[21] N. Aksuner, E. Henden, I. Yilmaz, A. Cukurovali, Dyes Pigments. 83 (2009) 211-217.
[22] Z. Yang, M. She, J. Zhang, X. Chen, Y. Huang, H. Zhu, P. Liu, J. Li, Z. Shi, Sens. Actuators B. 176 (2013) 482-487.

[23] L. Yang, W. Zhu, M. Fang, Q. Zhang, C. Li, Spectrochim. Acta A: Mol. Biomol. Spectrosc. 109 (2013) 186-192.
[24] M. Kumar, J.N. Babu, V. Bhalla, J. Incl. Phenom. Macrocycl. Chem. 66 (2010) 139-145.
[25] R. Azadbakht, S. Rashidi, Spectrochim. Acta A: Mol. Biomol. Spectrosc. . 127 (2014) 329-334.
[26] Z. Li, L. Zhang, X. Li, Y. Guo, Z. Ni, J. Chen, L. Wei, M. Yu, Dyes Pigments. 94 (2012) 60-65.
[27] M. Li, H.Y. Lu, R.L. Liu, J.D. Chen, C.F. Chen, J. Org. Chem. 77 (2012) 3670-3673.
[28] E. Hao, T. Meng, M. Zhang, W. Pang, Y. Zhou, L. Jiao, J. Phys. Chem. A. 115 (2011) 8234-8241.
[29] D. Ray, P.K. Bharadwaj, Inorg. Chem. 47 (2008) 2252-2254.
[30] J.S. Wu, W.M. Liu, X.Q. Zhuang, F. Wang, P.F. Wang, S.L. Tao, X.H. Zhang, S.K. Wu, S.T. Lee, Org. Lett. 9 (2007) 33-36.
[31] X.L. Tang, X.H. Peng, W. Dou, J. Mao, J.R. Zheng, W.W. Qin, W.S. Liu, J. Chang, X.J. Yao, Org. Lett. 10 (2008) 3653-3656.
[32] B. Tang, T. Yue, J. Wu, Y. Dong, Y. Ding, H. Wang, Talanta. 64 (2004) 955-960.
[33] J.H. Chang, Y.M. Choi, Y.K. Shin, Bull. Korean Chem. Soc. 22 (2001) 527-530.
[34] (a) J. Mao, L. Wang, W. Dou, X. Tang, Y. Yan, W. Liu, Org. Lett. 9 (2007) 4567-4570.
(b) K. Huang, H. Yang, Z. Zhou, M. Yu, F. Li, X. Gao, T. Yi, C. Huang, Org. Lett. 10 (2008) 2557-2560.
(c) Z. Zhou, M. Yu, H. Yang, K. Huang, F. Li, T. Yi, C. Huang, Chem. Commun. 29 (2008) 3387-3389.
[35] B. Tamami, H. Yeganeh, Polymer. 42 (2001) 415-420.
[36] M.Z. Kassaee, A.R. Bekhradnia, J. Biosci. Bioeng. 95 (2003) 526-529.
[37] N.C. Lim, S.V. Pavlova, C. Bruckner, Inorg. Chem. 48 (2009) 1173-1182.
[38] P. Alaei, S. Rouhani, K. Gharanjiga, J. Ghasemi, Spectrochim. Acta, Part A. 90 (2012) 85-89.
[39] R.M.F. Batista, S.P.G. Costa, M.M.M. Raposo, J. Photochem. Photobiol. A: Chem. 259(2013) 33-40.
[40] K. Rajendran, R. Perumal, J. Lumin. 130 (2010) 1203-1210.
[41] (a) X. Chen, T. Pradhan, F. Wang, J.S. Kim, J. Yoon, Chem. Rev. 112 (2011) 1910-1956.
(b) D. Liu, T. Pang, K. Ma, W. Jiang, X. Bao, RSC Adv. 4 (2014) 2563-2567.
(C) Z. Zhou, M. Yu, H. Yang, K. Huang, F. Li, T. Yi, C. Huang, Chem. Commun. 29 (2008) 3387-3389.
[42] (a) C.A. Parker, W.T. Rees, Analyst. 85 (1960) 587-600.
(b) Y. Gabe, Y. Urano, K. Kikuchi, H. Kojima, T. Nagano, J. Am. Chem. Soc. 126 (2004) 3357-3367.
[43] S. Goswami, A. K. Das, A.K. Maity, A. Manna, K.S. AichMaity, P. Saha, T.K. Mandal, Dalton Trans. 43 (2014) 231-239.
[44] P. Das, A. Ghosh, H. Bhatt, A. Das, RSC Adv. 2 (2012) 3714-3721.
[45] M. Mukherjee, B. Sen, S. Pal, M.S. Hundal, S.K. Mandal, A.R. Khuda-Bukhsh, P. Chattopadhyay, RSC Advances. 43 (2013) 19978-19984.
[46] A. Bekhradnia, E. Domehri, M. Khosravi, Spectrochim. Acta, Part A. 152 (2016) 18-22.
[47 J.R. Lakowicz, Principles of fluorescence spectroscopy, springer US. (2006).
[48] R.B. OrfãoJr, F. de Carvalho, P. Homem-de-Mello, F.H. Bartoloni, J. Braz. Chem. Soc. (2017) 1-9.
[49] (a) S. Goswami, A.K. Das, A.K. Maity, A. Manna, K. Aich, S. Maity, P. Saha, T.K. Mandal, Dalton Trans.43 (2014) 231-239.
(b) Y. Yang, H. Xue, L. Chen, R. Sheng, X. Li, K. Li, Chin. J. Chem. 31 (2013) 377-380.
(c) J. Zhang, L. Zhang, Y. Wei, J. Chao, S. Wang, S. Shuang, Z. Cai, C. Dong, Anal. Methods. 5 (2013) 5549-5554.
[50] P. Saluja, H. Sharma, N. Kaur, N. Singh, D.O. Jang, Tetrahedron. 68(2012) 2289–2293.
[51] L. K. Kumawat, N. Mergu, M. Asif, V. K. Gupta, Sens. Actuators B. 231 (2016) 847-859.
[52] Y.J. Jang, Y.H. Yeon, H.Y. Yang, J.Y. Noh, I.H. Hwang, C. Kim,Inorg. Chem. Commun. 33 (2013) 48–51.
[53] W. Zhu, L. Yang, M. Fang, Z. Wu, Q. Zhang, F. Yin, Q. Huang, C. Li, J. Lumin. 158 (2015) 38–43.
[54] S. Saha, P. Mahato, E. Suresh, A. Chakrabarty, M. Baidya, S. K. Ghosh, A. Das, Inorg. Chem. 51 (2011) 336-345.